Ultrasonic Hydrogel Biochemical Sensor System

Eunjeong Byun¹, Juhong Nam¹, Hyunji Shim¹, Esther Kim¹, Albert Kim², and Seunghyun Song¹

Abstract—In this work, we present a proof-of-concept hydrogel-based sensor system capable of wireless biochemical sensing through measuring backscattered ultrasound. The system consists of silica-nanoparticle embedded hydrogel deposited on a thin glass substrate, presenting two interfaces for backscattering (tissue/hydrogel and hydrogel/glass), which allows for system output to be invariant under the change in acoustic properties (e.g. attenuation, reflection) of the intervening biological tissue. We characterize the effect of silica nanoparticles (acoustic contrast agents) loading on the hydrogel's swelling ratio and its ultrasonic backscattering properties. We demonstrate a wireless pH measurement using dual modes of interrogations, reflection ratio and time delay. The ultrasonic hydrogel pH sensor is demonstrated with a sensing resolution of 0.2 pH level change with a wireless sensing distance around 10 cm.

I. INTRODUCTION

Continuous biochemical sensing of important physiological parameters is increasingly important in health-care. Implantable sensors, despite their invasiveness, typically provide direct access to the measurement sites and hence produce greater signal-to-noise ratio[1].

Hydrogels, i.e. crosslinked polymer networks that absorb water, are particularly suitable for implantable sensors as they do not require external power sources and exhibits reversible volume and shape response to a variety of chemical stimuli such as pH, ions, antigens, and glucose [2]. In addition, the physical response of hydrogels are typically mediated by the ioniziation of the functional groups without the involvements of enzymes or catalysts; thus, the lifetime of the hydrogel based systems can be much longer than those involving enzymatic reactions. For these advantages, there have been many studies to develop sensor systems using hydrogels as the

*This work was supported by the National Research Foundation of Korea, No. 2018R1C1B5086311.

sensing materials. For example, a passive MEMS LC glucose sensor system using the hydrogels to deflect the diaphragm was previously reported [3]. More recently, functionalization of hydrogel through the introduction of nanoparticles were explored; ferromagnetic nanoparticles were embedded to magnetically functionalize the hydrogel which served as the variable core for a planar inductor to enable wireless sensing [4] and silica nanoparticles were added to provide improved imaging contrast enabling the wireless measurement using an ultrasonic imaging equipment [5].

Ultrasonic interrogation of hydrogel remains an attractive method as it provides a long interrogation depth and small device dimensions with low complexity [5]. However, the ultrasonic scatterings in biological tissues are often complex and unpredictable; moreover, the echoes are known to be distorted by the intervening tissues between an ultrasonic probe and the target [6]. Although this limitation can be ameliorated by the use of an ultrasonic imaging equipment, a simple pulse-echo interrogation, a much more desirable alternative for a wearable readout system, is incompatible with a single block of silicagel.

In this paper, we present a proof-of-concept hydrogel-based sensor system capable of wireless biochemical measurement; by incorporating silica-embedded hydrogel on a glass substrate, backscattering occurs at two interfaces of tissue/hydrogel and hydrogel/glass. This sensor design enables a simple pulse-echo measurement enabling ultrasonic wireless biochemical sensing.

II. DESIGN AND OPERATION PRINCIPLE

A. Device Design

The device design is illustrated in Fig. 1. The implantable device consists of a pH sensitive hydrogel embedded with silica (SiO₂) nanoparticles (400 nm average size, U.S. Nanomaterials Research) deposited on a glass substrate. The silica nanoparticles are physically trapped by the small hydrogel meshes (typically in the order of tens of nanometers[2]) and they modulate both the acoustic impedance (Z_{gel}) and the attenuation coefficient (α_{gel}) of the hydrogel (equ. 1, 2); m_{SiO_2} is the total mass of the silica nanoparticles, c_{gel} is the speed-of-sound in the hydrogel, V_{gel} is the total volume of the hydrogel, and x is the w/v percentage of silica. The acoustic impedance of the hydrogel is a function of its volume, resulting in a different backscattering intensities [5]. Moreover, the attenuation coefficient of the gel is proportional to the concentration of the additional scattering agents (SiO_2).

¹E. Byun is with the Department of Electronics Engineering, Sookmyung Women's University, Seoul, Republic of Korea (eunjbyun@sookmyung.ac.kr)

¹J. Nam is with the Department of Electronics Engineering, Sookmyung Women's University, Seoul, Republic of Korea (dnu05024@sookmyung.ac.kr)

¹H. Shim is with the Department of Electronics Engineering, Sookmyung Women's University, Seoul, Republic of Korea (sim100428@sookmyung.ac.kr)

¹E. Kim is with the Department of Electronics Engineering, Sookmyung Women's University, Seoul, Republic of Korea (qhatt@sookmyung.ac.kr)

²A. Kim is a member of IEEE and currently an assistant professor at the Department of Electrical and Computer Engineering, Temple University, Philadelphia, PA 19122 USA (albertkim@temple.edu)

¹S. H. Song is an assistant professor at the Department of Electronics Engineering, Sookmyung Women's University, Seoul, Republic of Korea (shsong.ee@sookmyung.ac.kr)

Thus, the change in the hydrogel volume in response to the biochemical stimuli will change the backscattered ultrasound allowing wireless biochemical sensing.

$$Z_{gel} = \rho_{gel} \cdot c_{gel} = \left(\rho_{water} + \frac{m_{SiO_2}}{V_{gel}}\right) \cdot c_{gel}$$
 (1)

$$\alpha_{gel} = \alpha_{gn} + \alpha_{SiO_2} \propto x$$
 (2)

Fig. 1 shows the schematic illustration of the proposed sensor system. The sensor can be implanted in subcutaneous area and can be readily measured from a simple readout system consists of a ultrasonic element (e.g. a single transducer unit or an ultrasonic sensor utilizing piezoelectric micro-machined ultrasonic transducers (pMUT)).

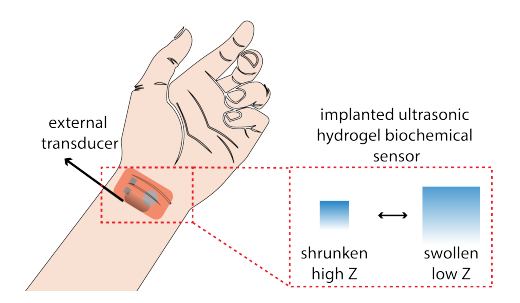


Fig. 1. Schematic illustration of the ultrasonic hydrogel biochemical sensor system $\,$

B. Operation Principle

The ultrasonic wave transmitted from the external transducer (P_{in}) travels through the biological tissue and is reflected by the sensor as illustrated in Fig. 2. The reflections occur at two interfaces; tissue/gel and gel/glass. The pressure of the two reflected waves are given by equ. 3 and equ. 4 (R_{gel}) is the reflection coefficient at the tissue/gel interface; α_{tissue} and α_{gel} are the attenuation coefficients of the tissue and the hydrogel; d_{tissue} and d_{gel} are the thicknesses of the tissue and the hydrogel).

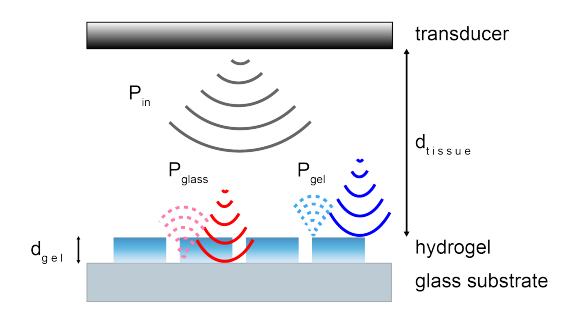


Fig. 2. Operation principle of ultrasonic hydrogel biochemical

$$P_{gel} = R_{gel} \cdot e^{-2\alpha_{tissue} \cdot d_{tissue}} \cdot P_{in}, \quad R_{gel} = \left| \frac{Z_{gel} - Z_{tissue}}{Z_{gel} + Z_{tissue}} \right| \quad (3)$$

$$P_{glass} = (1 - R_{gel}) \cdot e^{-2\alpha_{tissue} \cdot d_{tissue}} \cdot e^{-2\alpha_{gel} \cdot d_{gel}} \cdot P_{in}$$
 (4)

Because the attenuation in the intervening tissues can vary under different factors (e.g. transducer location, hydration, muscle movements, and etc.), directly inferring the hydrogel's thickness (and hence the local biochemical information) from the intensity of the reflected wave (P_{gel}) alone is difficult and likely unreliable. On the other hand, equation 5 indicates that the relative ratio between the reflected echos at tissue/gel and gel/glass interface should be independent of the intervening tissue's acoustic parameters. Alternatively, the gel thickness to be inferred from time-of-flight measurement (equ. 5, c_{gel} is the speed of sound in the hydrogel).

$$\frac{P_{gel}}{P_{glass}} = \frac{R_{gel}}{(1 - R_{gel}) \cdot e^{-2\alpha_{gel} \cdot d_{gel}}}, \qquad \Delta t = \frac{2d_{gel}}{c_{gel}}$$
(5)

III. RESULTS & DISCUSSIONS

A. Device Fabrication

The fabrication process of the ultrasonic hydrogel sensor is illustrated in Fig. 3. Firstly, the glass substrates were pre-treated in a 10 vol % solution (in acetone) of organosilane coupling agent, γ -methacryloxypropyl trimethoxysilane (γ -MPS, Sigma-Aldrich), for 1 hour and dried in an oven (120 C°) for 1 hour. A thin layer of silica loaded hydrogel (10 w/v%) was deposited on the pre-treated substrate (Fig. 3a) following the procedure described by Ding [7]. The resulting sample of silica-loaded hydrogel on glass substrate was completely dehydrated (Fig. 3b). The hydrogel film was then cut into squares of $(500 \ \mu\text{m})^2$ with 500 μ m spacing using a CO₂ laser cutter (Fig. 3c-d). The patterns were introduced to improve the response time and the reversibility by reducing the strain build-up in the gel [4]. The patterned hydrogel sensor was then immersed in DI water to extract the burnt polymers and unreacted monomers overnight. Fig. 3e shows the hydrogel patterns in two magnifications $(8 \times \text{ and } 25 \times, \text{ Leica MZ10F}).$

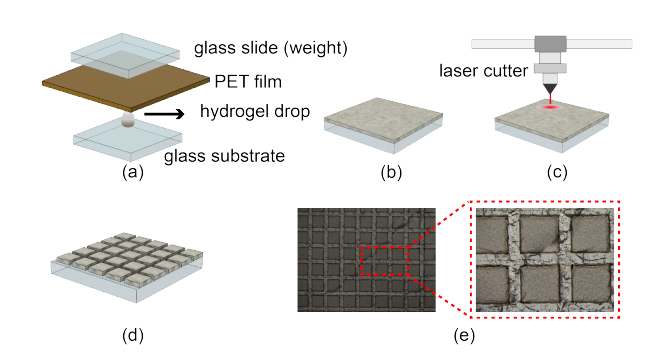


Fig. 3. Fabrication process: (a-b) silica-loaded hydrogel deposition on glass substrate (c-d) laser patterning of the hydrogel (e)optical photographs of the fabricated sample.

B. Effects of Particle Loading on Hydrogel Swelling Behaviors

While nanoparticle loading can increase the scattering/reflection at the tissue/gel boundary by modulating the hydrogel density (equ. 1), high loading concentrations can degrade the swelling behavior of the hydrogel. Thus, we investigated how the pH sensitive hydrogel swelling behaviors are affected by the particle loading. For this, we firstly prepared hydrogel cuboids $(5 \times 5 \times$ $3 mm^3$) with three different silica loading concentrations of 0, 5, and 10 %. The mixed pre-gel solutions were poured into the mold and removed after polymerization $(\approx 10 \text{ minutes})$. The silica-loaded hydrogel cuboids were then immersed in buffer solutions (Deajung Chamicals, Korea) with different pH ranging from 3 to 9 for 24 hours to allow the hydrogel volumes to equilibrate. Fig. 4a-d show the optical photographs of the hydrogel (10 w/v %) at four different pH levels of 3, 4, 6, and 9. The normalized dimensions of the hydrogels at different pH (normalized by the dimension at pH 3) are summarized in Fig. 4e. The observed hydrogel swelling behaviors were similar to the previous reports with a sharp volume change between pH of 3 to 6 [8], [9]. The swelling behaviors remained unaffected by the embedded silica loading up to 10 w/v\% with 4-fold (1.6^3) maximum volume increase.

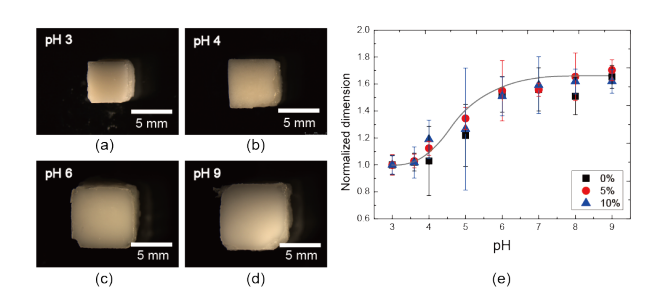


Fig. 4. Swelling behaviors of silica-loaded hydrogel with different loading concentrations: (a-d) Optical photographs of silica-loaded hydrogel (10 w/v%) at different pH (all scale bars are 5 mm long). (e) Normalized dimensions of the silica-loaded hydrogels at different pH

C. Ultrasonic Backscattering Characterization of Silicaloaded Hydrogel

To preliminary study the effect of different silica loading concentrations, we prepared 2% agarose gels (7 mm thick) with different silica loading concentrations. We chose agarose gel instead of pH sensitivy hydrogel to minimize the uncertainty introduced to the silica particle concentration during characterizations. Since, the acoustic properties of the nanoparticle loaded gels are mostly determined by the concentrations of the loaded particles[10], agarose gel can be used to estimate the effect of silica-loading on pH sensitive gel.

The experimental setup is schematically illustrated in Fig. 5a. A custom-built PZT transducer (2.3 MHz,

Mide Technology, US) was placed in a water tank. The samples, silica-loaded gels with different concentrations on glass substrates, were placed at the other end of the tank about 15 cm from the transducer. The transducer was driven in a pulsed mode ($N=5,1~\mathrm{kHz}$ repetition rate) at its resonance frequency by a function generator connected to a power amplifier (240L, E&I, US). The transducer output was monitored using an oscilloscope.

Fig. 5b-c show the pulse-echo waveforms measured by the transducer of a control sample (no gel) and 10% silica gel. A clear reflection from the hydrogel surface is observed in Fig. 5c whereas only one reflection at the glass surface is observed in Fig. 5b. The reflection interfaces were identified by using the time-of-flight. The measured signals were processed using a 7th order Butterworth bandbpass filter with passband of 1-3.9 MHz to remove the RF interference and the DC fluctuation. The maximum peak-to-peak were used to calculate the peak pressure of the reflected waves. The time delay of about 9 μ s, corresponding to $2d_{gel}=14$ mm, is in a good agreement with the gel thickness of 7 mm.

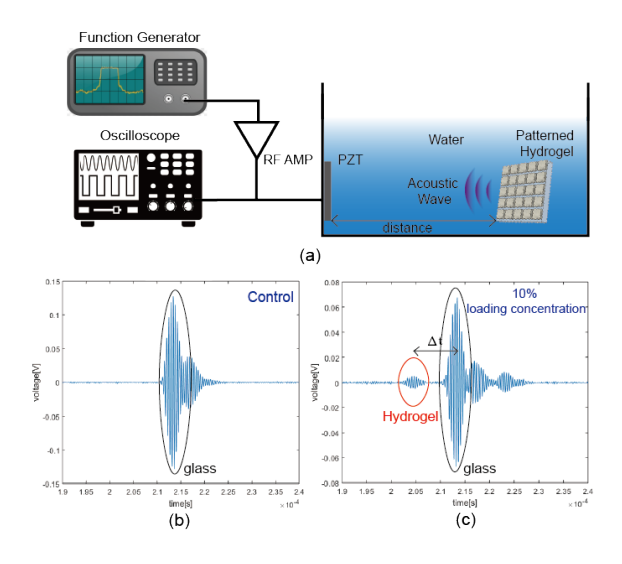


Fig. 5. Ultrasonic backscattering characterization of silicaloaded hydrogel (a) experimental setup (b-c) representative pulse-echo graphs from control (no gel) and 10 % silica loading concentrations, respectively.

The backscattering measurement results are summarized in Fig. 6. The magnitude of reflected waves at the gel surface increased with the increasing loading concentrations (Fig. 6a); the tail-off is likely due to the decrease in acoustic velocity compensating for the increase in the density [10]. On the other hand, the peak pressure of waves reflected at the glass substrate decreased exponentially with increasing silica concentration due to the presence of added scattering sites (Fig. 6b) [11]. The time difference between the first and the second echoes were relatively constant for all samples (Fig. 6c). Finally, the ratios between the reflected echoes from the two interfaces (P_{gel}/P_{glass}) at different loading concentrations exponentially increases (mostly due to

the contribution of attenuation) as a function of silica concentration (Fig. 6d).

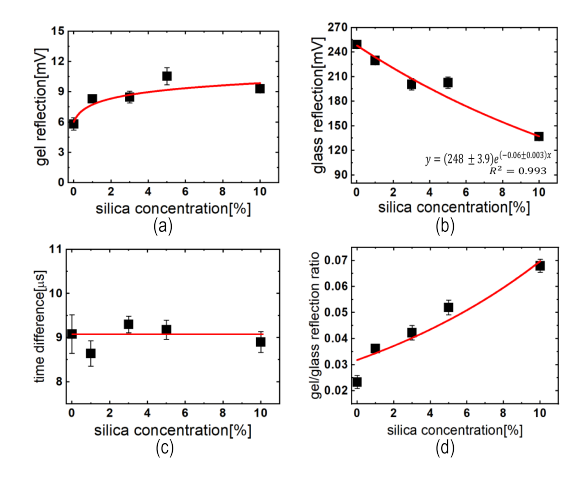


Fig. 6. Evolution of backscattered ultrasonic echoes under different loading concnetrations (a) transducer voltage output due to the reflection at the water/gel interface (b) transducer voltage output due to the reflection at the gel/glass interface (c) the time delay (Δt) for different loading concentrations for the hydrogels with the same thicknesses (d) gel/glass reflection ratio as a function of silica loading concentration

D. Ultrasonic Hydrogel Sensor for Wireless pH Measurement.

For pH measurement testing, the ultrasonic hydrogel sensor ($5 \times 5 \times 2$ mm³) was placed 7 cm away from the transducer. The sensor response were measured in both the ratio of reflection and the time difference between the reflections (Fig. 7). The reflected wave at the gel surface ((P_{gel} , black curve) remained relatively constant independent of pH, consistent with the result presented in Fig. 6a. At the same time, the pressure of the waves reflected by the glass substrate (P_{glass} , red curve, Fig. 7a) diminishes with increasing pH due to the increased attenuation; while the attenuation coefficient itself likely decreases with increasing hydrogel volume, the gel thickness (increased path) appears to be the more dominant factor, resulting in increased attenuation.

Fig. 7b shows the reflection ratio (P_{gel}/P_{glass}) and the time delay as a function of pH. The reflection ratio decreases as pH increases; the gel reflection is relatively independent of pH, but the glass reflection decreases with increasing pH. Time delay (Δt) is more straightforward as it is linearly proportional to the gel thickness. The maximum time delay increases about 1.7 times when pH is change from 3 to 7; this is consistent with the normalized dimension change measured from pH sensitivity gel of 1.7 as well (Fig. 4e). The resolution of the sensor, assuming measurement resolution defined by 2σ (stdev), is about 0.2 change in pH level.

IV. CONCLUSION

The proof-of-concept device presented in this study successfully measures pH with a working distance of

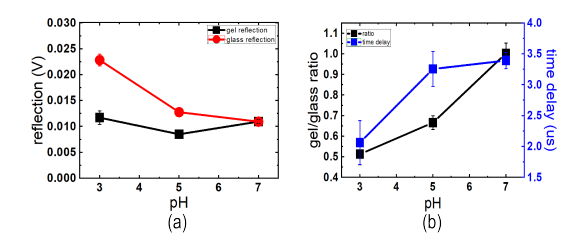


Fig. 7. Wireless pH sensing using ultrasonic hydrogel biochemical sensor (a) gel and glass reflection as a function of pH (b) reflection ratio (P_{eel}/P_{elass}) and time delay as a function of pH

 $\approx 10~\rm cm$ using moderately weak acoustic intensity (< $200~\rm mW/cm^2).$ In addition, the system can be applied to sense different analytes by incorporating hydrogel sensitive to different stimuli. Looking forward, further reduction of the sensor dimension will be required for a realistic application of the sensor system especially in the thickness, which will make the time delay measurement difficult as two reflected waves overlap in the time domain. Moreover, the sensor performance as a function of volume of the sensing bulk will require further investigations.

References

- A. Darwish and A. E. Hassanien, "Wearable and implantable wireless sensor network solutions for healthcare monitoring," Sensors, vol. 11, no. 6, pp. 5561–5595, 2011.
- [2] R. A. Siegel, Y. Gu, M. Lei, A. Baldi, E. E. Nuxoll, and B. Ziaie, "Hard and soft micro-and nanofabrication: An integrated approach to hydrogel-based biosensing and drug delivery," Journal of Controlled Release, vol. 141, no. 3, pp. 303–313, 2010.
- [3] M. Lei, A. Baldi, E. Nuxoll, R. A. Siegel, and B. Ziaie, "A hydrogel-based implantable micromachined transponder for wireless glucose measurement," Diabetes Technology & Therapeutics, vol. 8, no. 1, pp. 112–122, 2006.
- [4] S. Song, J. Park, G. Chitnis, R. A. Siegel, and B. Ziaie, "A wireless chemical sensor featuring iron oxide nanoparticleembedded hydrogels," Sensors and Actuators B: Chemical, vol. 193, pp. 925–930, 2014.
- [5] J. Park, A. Kim, H. Jiang, S. H. Song, J. Zhou, and B. Ziaie, "A wireless chemical sensing scheme using ultrasonic imaging of silica-particle-embedded hydrogels (silicagel)," Sensors and Actuators B: Chemical, vol. 259, pp. 552–559, 2018.
- [6] K. K. Shung and G. A. Thieme, Ultrasonic scattering in biological tissues. CRC press, 1992.
- [7] Z. Ding, A. Salim, and B. Ziaie, "Squeeze-film hydrogel deposition and dry micropatterning," Analytical chemistry, vol. 82, no. 8, pp. 3377–3382, 2010.
- [8] M. Quesada-Pérez, J. A. Maroto-Centeno, J. Forcada, and R. Hidalgo-Alvarez, "Gel swelling theories: the classical formalism and recent approaches," Soft Matter, vol. 7, no. 22, pp. 10536-10547, 2011.
- [9] M. Lei, Y. Gu, A. Baldi, R. A. Siegel, and B. Ziaie, "Highresolution technique for fabricating environmentally sensitive hydrogel microstructures," Langmuir, vol. 20, no. 21, pp. 8947–8951, 2004.
- [10] A. Cafarelli, A. Verbeni, A. Poliziani, P. Dario, A. Menciassi, and L. Ricotti, "Tuning acoustic and mechanical properties of materials for ultrasound phantoms and smart substrates for cell cultures," Acta biomaterialia, vol. 49, pp. 368–378, 2017.
- [11] D. O. Thompson and D. E. Chimenti, Review of progress in quantitative nondestructive evaluation. Springer Science & Business Media, 2012, vol. 18.